Ocean Engineering 147 (2018) 476–487

Contents lists available at ScienceDirect

Ocean Engineering

journal homepage: www.elsevier.com/locate/oceaneng

Modeling the sediment dynamics in the gulf of Urabá, colombian Caribbean sea

Carlos A. Escobar [a,*], Liliana Velásquez-Montoya [a,b]

[a] Departamento de Ingeniería Civil, Universidad EAFIT, Carrera 49 # 7 Sur 50, Medellín, Colombia
[b] Department of Civil, Construction and Environmental Engineering, North Carolina State University, 2501 Stinson Drive, Raleigh, NC, 27695, USA

ARTICLE INFO

Keywords:
Sediment transport model
Atrato River plume
Delft3D
Data scarcity
Estuarine dynamics

ABSTRACT

The potential of the gulf of Urabá to hold a multi-purpose port motivated a sediment dynamics study to describe the seasonal sediment concentration patterns in this tropical region. Challenges addressed in this study include a complex three-dimensional flow pattern in a tropical estuary and the lack of *in-situ* measurements. To overcome such challenges, this study completed: (i) Measurements of suspended sediment concentrations during two climatic seasons and an extreme event (2010–2011); (ii) Definition of boundary conditions from global databases; (iii) Qualitative analysis of sediment concentrations from satellite imagery; and (iv) integration of the previously mentioned steps to build a process-based 3D sediment transport model. Seasonal patterns of suspended sediment concentrations were identified and corroborated by the agreement between model results, satellite imagery and field measurements. During the calm rainy season, the Atrato River turbid plume extends northward and dominates the sediment dynamics in the gulf. On the other hand, during the dry season and extreme events, bed transport is enhanced and the river's plume and the littoral drift shift southwards.

1. Introduction

The strategic location of the Gulf of Urabá in the southernmost portion of the Caribbean Sea, as well as, the export-quality banana produced in the region, make this tropical estuary of particular interest for governmental plans related to the construction of a multi-purpose port and an interoceanic channel (BIRD, 2010; Cámara de Comercio de Medellín para Antioquia, 2006; Hubach, 1930). To achieve these development plans, understanding the sediment dynamics of the gulf has become a priority, especially because it could lead to a long-term solution to sedimentation and erosion problems in the region. The former occurring in Bahia Colombia and the navigational channels in the deltas of the Atrato and León Rivers, and the latter taking place on the east coast of the gulf, where erosion rates up to 0.5 m/yr have been reported (Correa and Vernette, 2004; Posada and Henao, 2008; Velasquez and Rave, 1996). However, the lack of measurements or a systematic program to collect oceanographic and atmospheric data in the gulf, including the Atrato River delta, increases the challenges to complete sediment dynamic studies in the region.

The factors controlling the sediment dynamics in coastal and estuarine zones are both naturally and anthropogenically originated (Stanica et al., 2007; Syvitski and Milliman, 2007; Van Rijn, 1993; Walling, 2006). Within the Gulf of Urabá, forces due to river discharges, waves, winds and density gradients are responsible for the hydrodynamics and sediment transport (Bernal et al., 2005; Chevillot et al., 1993; Escobar, 2011; Montoya and Toro, 2006; Velasquez and Escobar, 2012). The human impacts have also been studied in this area by Correa and Vernette (2004) and Correa et al. (2005), who identified the relocation of the mouth of the Turbo River and the unplanned construction of groins and seawalls as anthropogenic causes of erosion.

The regional and local importance of the Gulf of Urabá have led to multiple studies performed to identify its sediment circulation, some of them based on satellite imagery (Molina et al., 1992), turbidity measurements (Chevillot et al., 1993), and seabed granulometric parameters (Álvarez and Bernal, 2007). Despite the importance of these studies, they could not cover the 3D circulation structure of the gulf. Later, Montoya (2010) presented a numerical model which overcame that restriction, but the scarce measurements of currents, suspended sediment concentration (SSC) and the disregard of wave effects limited the evaluation of the modeled sediment dynamics.

This study aims to describe seasonal sediment concentrations patterns in the Gulf of Urabá by means of a 3D sediment transport model that includes the influence of the wind, waves, tides, river discharges and density gradients. This model was built over a validated hydrodynamic

* Corresponding author.
E-mail addresses: carloses@eafit.edu.co (C.A. Escobar), lvelas17@eafit.edu.co (L. Velásquez-Montoya).

https://doi.org/10.1016/j.oceaneng.2017.10.055
Received 30 April 2013; Received in revised form 26 October 2017; Accepted 29 October 2017
Available online 10 November 2017
0029-8018/© 2017 Elsevier Ltd. All rights reserved.

model of the study area (Escobar et al., 2015). To verify the reliability of the sediment transport model, calibration and validation were completed through quantitative comparisons at 314 locations, where SSC samples were obtained in three separate field campaigns. Moreover, the model was qualitatively validated by comparing its results with observed sediment concentration patterns on satellite images.

2. Study area

The Gulf of Urabá is located in the southernmost zone of the Caribbean Sea, as shown in Fig. 1. Its northwest cape known as Cabo Tiburón delimits the Republics of Colombia and Panama, just where South America begins. The gulf's maximum depth reaches 75 m at the north and progressively reduces along its central axis until the southernmost area called Bahia Colombia, which has maximum depths of 25 m. The gulf's width varies between 49 and 6 km, its narrowest area is the result of the constriction generated by the Atrato River bird foot delta, which drains in oceanic waters through seven main mouths.

According to the classification by Galloway (1975), the Atrato delta is river-dominated and has a major role in the hydrodynamics and sediment transport in the gulf (Escobar, 2011; Montoya and Toro, 2006). This river drains one of the rainiest regions of the world with an average annual precipitation that exceeds 12500 mm (Mesa et al., 1997) and a drainage area of 35000 km^2. Measurements performed within this study captured Atrato River discharges between 4000 and 5000 m^3/s and SSC up to 120 mg/l. A summary of the discharge and solid input from Atrato's main mouths is presented in Fig. 1, where the relative contribution of El Roto, Leoncito and Matuntugo distributaries is also shown. These values constitute the only measurements available on river discharges. About 22 smaller rivers than the Atrato River also discharge their water in the gulf, among them, the León, Turbo and Acandí stand out, the first two are located on the east coast.

The migration of the Intertropical Convergence Zone (ITCZ) generates two seasons in the gulf (Poveda and Mesa, 1997). During the rainy season, between May and November, the ITCZ is located over the gulf causing high rates of precipitation of about 200 mm/month (CIOH, 2010) and weak winds from different directions. From December to April, during the dry season, the ITCZ is located to the south of the gulf, generating northerly trade winds that can reach 9.4 m/s in February (Chevillot et al., 1993).

The gulf has a micro-tidal regime with mixed semidiurnal tides; the tidal range at the northern boundary is less than 0.5 m. Although there is not a complete characterization of the wave climate in the region, it is known to be seasonal. Data from the WAVEWATCH III® Model (WWIII) indicates a dominant north direction, wave periods of about 6 s and mean significant wave heights (Hs) about 0.8 and 1.6 m during the rainy and dry seasons respectively. In the northern part of the gulf, waves depend on weather conditions out in the Caribbean Sea (swell), while in the south they are mainly generated by local meteorological conditions (Osorio et al., 2010). The same authors estimated the wave height with a 35-year return period to be around 5 m high. The seasonality of waves and winds influences the currents in the region and the discharge of the Atrato River creates a stratified circulation during calm conditions that is modified under energetic events (Escobar et al., 2015).

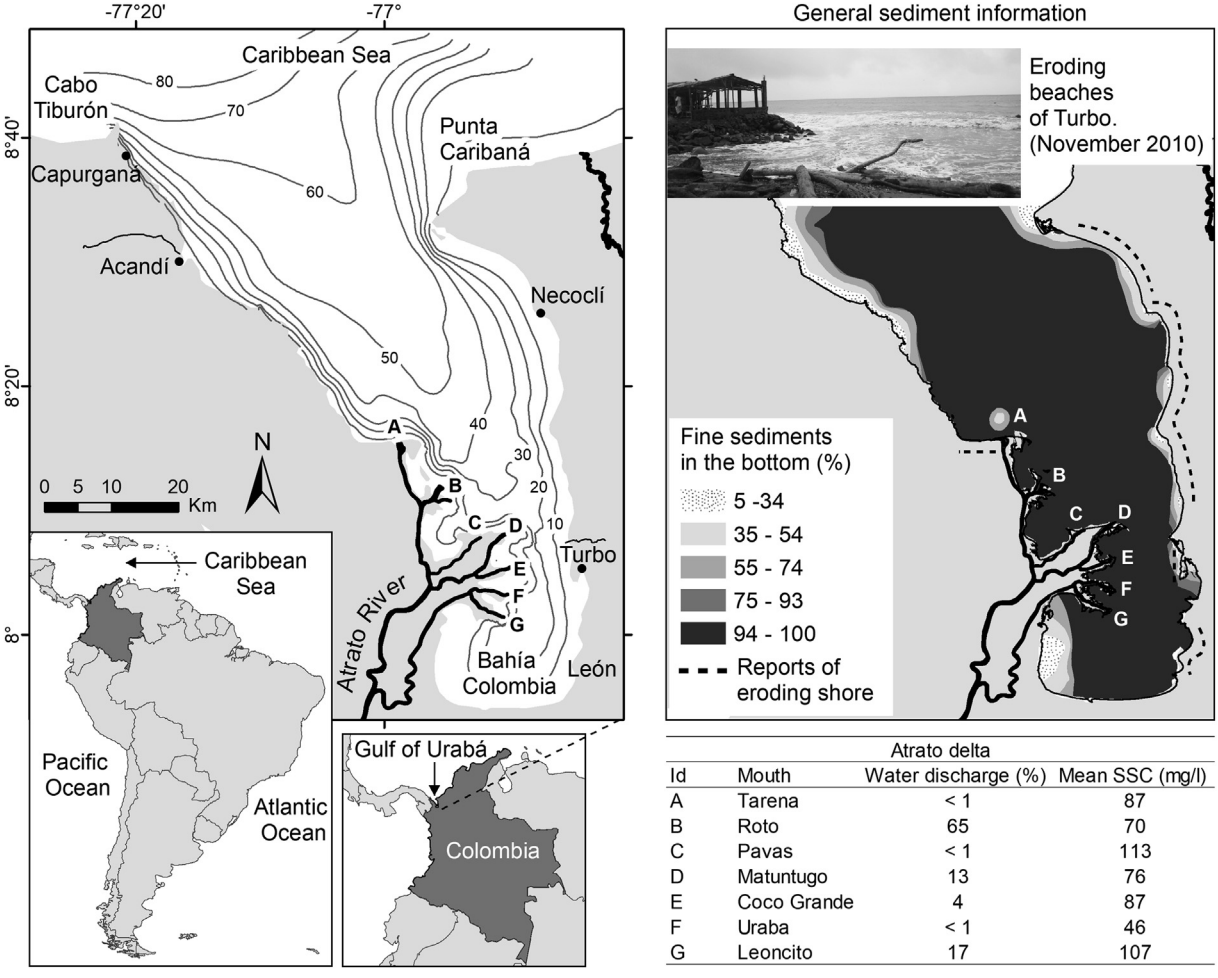

Atrato delta

Id	Mouth	Water discharge (%)	Mean SSC (mg/l)
A	Tarena	< 1	87
B	Roto	65	70
C	Pavas	< 1	113
D	Matuntugo	13	76
E	Coco Grande	4	87
F	Uraba	< 1	46
G	Leoncito	17	107

Fig. 1. Location, bathymetry and distribution of fine sediments in the bed of the Gulf of Urabá (Modified from Thomas et al., 2007). Summary of the Atrato River measurements in three field campaigns. Capital letters in the top panels serve as identifiers of each mouth of the Atrato River delta.

The seabed of the gulf is composed primarily of fine sediments (Fig. 1). Nevertheless, coarser particles are found in shallow regions, especially on the northwest coast and the most protected area of Bahia Colombia, where non-cohesive sediments constitute more than 70% of the bed (Thomas et al., 2007). Coastal erosion problems are commonly found on the east coast of the gulf, whereas continuous dredging is required in the Atrato delta and Bahia Colombia (Fig. 1) due to the high and still unknown rates of sedimentation.

3. Data

3.1. Field data: SSC, discharge of the Atrato River, thermohaline conditions, waves and water levels

Measurements of instantaneous SSC were conducted in three separate oceanographic cruises in April 2010, November 2010 and November 2011. More than 1400 km were traversed in a vessel during the three field campaigns, which covered two distinct climatic seasons and one extreme weather event. For each field campaign, measurements of instantaneous SSC were made in the gulf and at the seven main distributaries of the Atrato River as close as possible to the river's mouths, for a total of 314 samples and 83 samples, respectively.

Field campaigns were designed to capture the spatial variability of the SSC. The basis for these designs was the spatially varying sediment concentrations that can extend past the nearshore region, resulting from the influence of several external forcings driving the dynamics of the gulf (Escobar et al., 2015). Measurements of SSC were made instantaneously at the predefined stations indicated in Fig. 2. This method renders a considerable amount of spatially distributed information at the expense of temporal resolution. During the last field campaign in November 2011, the number of SSC samples was increased along the shallow areas of the east coast and the Atrato delta to focus data acquisition in areas with high SSC gradients due to wave processes and river outflows.

Measurements of SSC were completed by mechanical sampling using a Niskin bottle. In each campaign, water samples were collected from various locations covering different water depths, tidal and lunar phases, and climatic seasons. Sediment concentration was determined (i) directly by filtering water samples using fiber-glass filters GC50 with a pore size of 0.5 μm following the standard protocol 2540 (American Public Health Association et al., 1998); and (ii) indirectly by measuring turbidity with a WPA TU140 turbidimeter.

To define boundary conditions for the model, measurements of the discharge of the Atrato River in the west coast and the thermohaline distribution along the northern boundary of the study area were completed. Instantaneous river and thermohaline forcings were measured once per field campaign due to limited availability of Acoustic Doppler Current Profilers (ADCP) and Conductivity, Temperature and Depth profilers (CTD). Discharges and SSC of the Atrato River mouths were measured one at the time. Therefore, these variables are influenced by changes in the river conditions that could have occurred within the sampling periods ranging from a few hours up to one day. Measurements of the discharge of the smaller Atrato River distributaries was completed as far as possible from the main distributary. Nevertheless, this was not always guaranteed due to navigational restrictions in shallow waters. The vertical distribution of salinity and temperature was measured at four stations distributed along the gulf's northern boundary, as shown in Fig. 2.

An upward-looking ADCP was deployed for a three-month period at a depth of 18 m, at the location indicated by a star in Fig. 2. The ADCP continuously recorded water levels and directional waves from August 2010 to November of 2010 including the model's validation period (see section 4.4) and the time when Hurricane Tomas passed through the

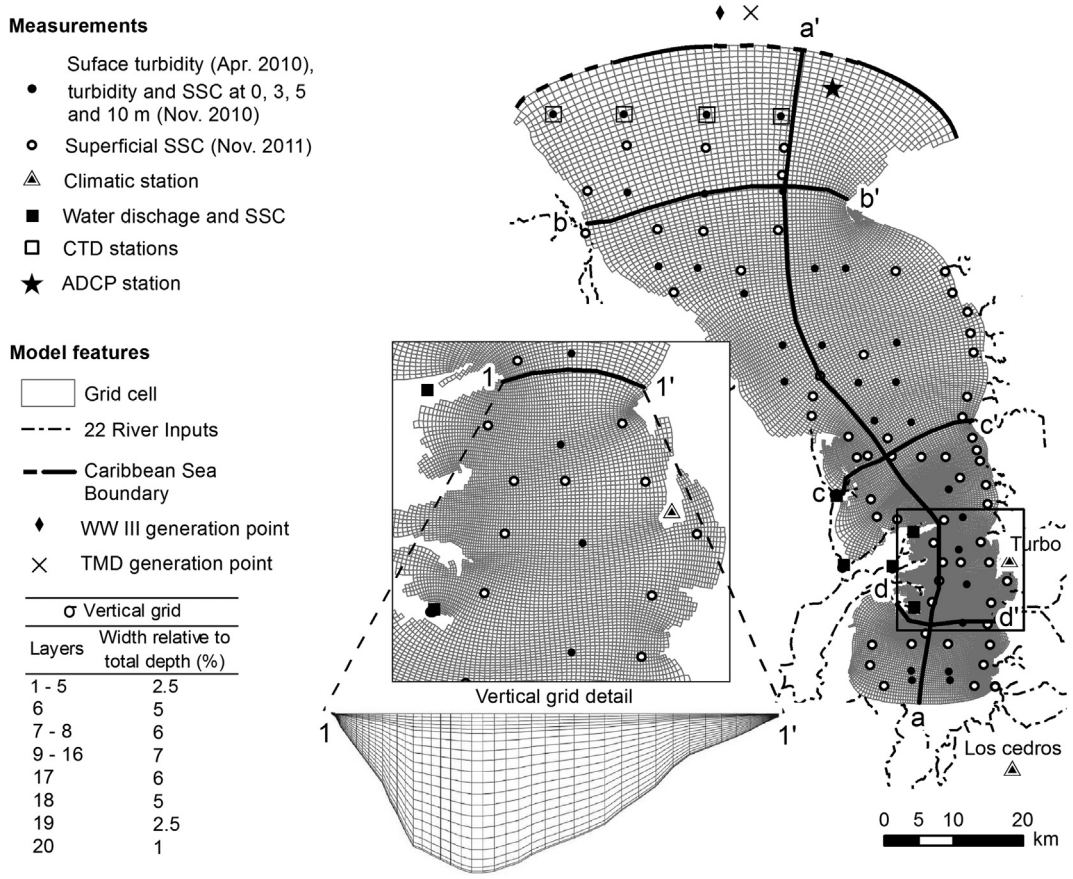

Fig. 2. Model domain and location of field measurements for all field campaigns.

Caribbean. Water levels were recorded every 20 min while waves every 3 h with a burst time of 20 min and a ping period of 0.5 s. The deployment of this instrument was not possible during the first and third oceanographic cruises. Nevertheless, the data obtained during the deployment period was useful to validate secondary sources of boundary conditions (i.e. global models) used when field measurements were unavailable (sections 3.2 and 4.4).

Velocity profiles along multiple cross sections were measured in the gulf. Additionally, temperature and salinity profiles were measured at the stations shown in Fig. 2. This data was used to investigate the hydrodynamics of the region and to evaluate the performance of the hydrodynamic model that constitutes the base of the sediment transport model introduced in this study. Details on these measurements and the hydrodynamics of the gulf are presented in Escobar et al. (2015).

3.2. Global models and pre-existent databases: tides, waves, atmospheric conditions, bathymetry and sea bed composition

Data from global models and pre-existing databases were used as boundary conditions for the numerical model when observations were unavailable. Examples of global model data include wave and tide conditions at the northern boundary of the gulf. Waves were obtained from the third generation wave model WWIII (Tolman, 1997) at the location indicated with a cross in Fig. 2. Tides were extracted from the Tide Model Driver (TMD) (Egbert and Erofeeva, 2002) at the point marked with a diamond in the same figure.

Atmospheric variables such as air temperature, relative humidity, short wave radiation, atmospheric pressure and wind were obtained from local meteorological stations located in Turbo and Los Cedros (see triangles in Fig. 2). The inland location of the stations is expected to influence wind records by reducing their magnitude due to enhanced friction over land. However, these stations are the only *in-situ* source of meteorological conditions. Data gaps in the time-series of wind records were filled with data from the NASA's Quik Scatterometer (QuikSCAT) and Advanced Scatterometer (ASCAT). Relative humidity, air temperature, pressure, and cloud cover percentage were obtained from the National Center for Atmospheric Research (NCAR) (Kalnay et al., 1996) and the North American Regional Reanalysis (NARR) (Mesinger et al., 2006) projects.

The bathymetry was digitized from the nautical chart of the Colombian General Maritime Direction (DIMAR). The discharges of minor tributaries were determined through hydrological balances and the HidroSIG software (Velez et al., 2000). Seabed composition was defined from the sediment samples taken in 2003 and 2004, and processed by Thomas et al. (2007).

4. Numerical model

The Delft3D modeling platform developed by WL|Delft Hydraulics (Roelvink and Van Banning, 1994) was used to build the sediment transport model for the Gulf of Urabá. The software suite provides built-in coupling of hydrodynamics, waves and sediment transport. The hydrodynamic model solves the Navier Stokes equations for an incompressible fluid under the shallow water, Boussinesq and hydrostatic pressure assumptions (Deltares, 2012). The turbulent fluctuations are included through Reynolds stresses and related to the Reynolds-averaged flow by a κ-ε turbulence closure model (Uittenbogaard et al., 1992). The model accounts for the effects of tides, density gradients, river discharges, wind drag and waves.

Waves are computed through the third-generation model Simulating WAves Nearshore (SWAN) (Booij et al., 1999). The built-in online coupling of SWAN and Delft3D allows accounting for wave-current interaction processes, which are particularly important for sediment dynamics, like mass flux due to waves, turbulence increase due to breaking waves and enhancement of bed shear stresses (Reniers et al., 2004). Validation of the performance of the hydrodynamic and wave modules was completed in a previous phase of this study (Escobar et al., 2015). The sediment transport model presented in this paper builds upon that work.

The computation of SSC in the model depends on the interaction of currents, waves and sediment availability from rivers and bed composition. SSC are solved by the three-dimensional advection-diffusion equation for two sediment types: cohesive ($d_{50} < 63$ μm) and non-cohesive ($d_{50} = 150$ μm). The spatial availability of these types of sediments in the seabed is included in the model according to the distribution shown in Fig. 1.

Settling velocity of non-cohesive particles is calculated based on their size using Van Rijn's (2007b) formulation. On the other hand, settling velocity of cohesive sediments was calibrated in two sub-regions differentiated by their exposure to wave action (see Section 4.3). This spatially-varying calibration was completed to partially account for processes that are not fully implemented in Delft3D, like flocculation and breakup of sediment flocs due to variable turbulence and salinity.

The exchange of sediments between the bed and the flow is solved by means of mathematical formulations that compute the erosive or depositional response of the bottom to bed shear stress, upward diffusion, and settling velocity. For cohesive sediments, the fluxes between the bed and the flow are calculated with the Partheniades-Krone formulations (Partheniades, 1965). For non-cohesive particles, the same process is modeled using Van Rijn (2007a) sink and source terms acting above a reference height that separates suspended and bed transports.

The solution of the model through a finite difference scheme (Leendertse, 1967; Leendertse et al., 1973; Stelling, 1983) required the construction of a curvilinear grid with 21961 cells. The spatial resolution of the grid varies between 37 m in the narrowest region of the gulf and 1200 m in the northern boundary. The grid has finer cells near the Atrato River delta where more complicated dynamics were anticipated. To capture the 3D dynamics of the gulf, a Sigma grid (Phillips, 1957) with 20 depth-variable layers was used in the vertical direction. The near-surface and -bottom layers are the thinnest layers aimed to capture the Atrato's plume and near-bed transport. All model's modules (flow, wave and sediment transport) used the same spatial discretization. Details of the grid and locations of boundary forcings are presented in Fig. 2.

4.1. Spatial sensitivity analysis

To identify the most relevant factors in the computation of SSC, spatial sensitivity analyses to numerical and physical parameters were completed under relatively calm weather conditions. Pairs of simulations including and excluding external forcings or considering different values of the parameters were run (i.e. with and without waves, horizontal eddy viscosity set to 1, 10 and 100, etc.). The relevance of the parameters was estimated at each grid cell based on the difference in modeled SSC for each pair of simulations. As a result, the method confirmed the spatial extent in which each parameter had the most influence.

Fig. 3 shows the discrepancies of SSC obtained from pairs of simulations involving three of the most important forcings in the gulf: waves, thermohaline processes and the discharge of the Atrato River. Positive differences (dark colors) indicate an increase in SSC caused by the external forcing, while negative values imply an increase in SSC when neglecting the forcing.

The inclusion of waves in the model resulted in an overall increase of SSC in the study area. As expected, wave effects are enhanced in shallow waters along the coast and in the Atrato River delta, where sediment transport capacity is higher due to wave-bottom interaction and wave breaking. On the other hand, under the calm conditions considered in this sensitivity analysis, the southernmost part of the gulf (Bahia Colombia) seems to be well protected from wave's action. Nonetheless, it should be noted that high-energy events, can disrupt the dynamics in Bahia Colombia (Osorio et al., 2010; Escobar et al., 2015).

Density gradients (thermohaline forcing) and the Atrato River discharge are highly relevant in the advection processes near the Atrato

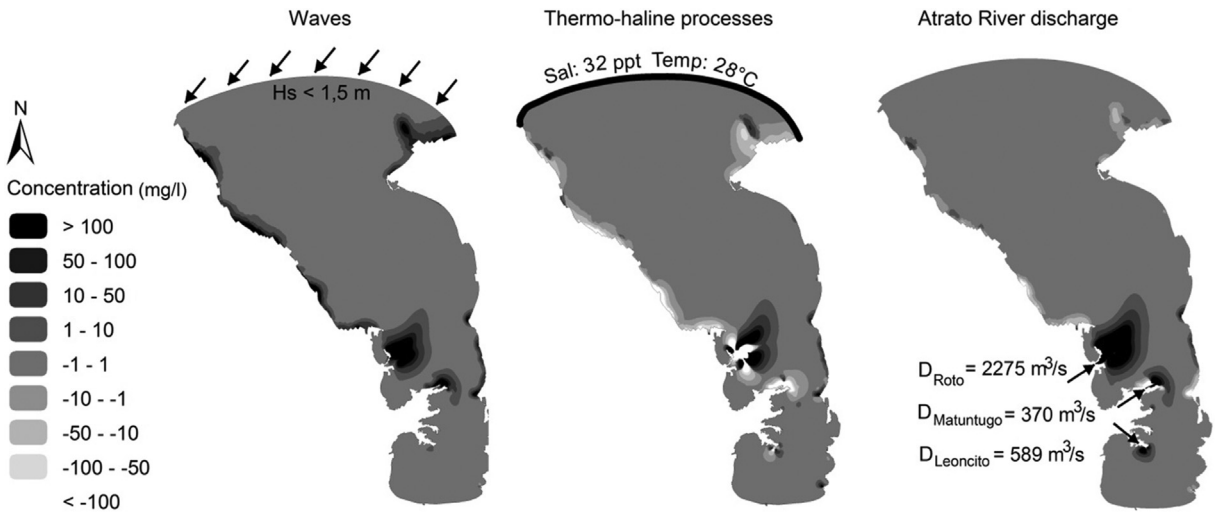

Fig. 3. Spatial variation of waves (left), thermohaline processes (middle) and Atrato River (right) effects on SSC in the Gulf of Urabá. Positive concentrations denote an increase in SSC gained when including each forcing in the model, while negative concentrations depict a decrease in SSC when neglecting the effect of each phenomenon in the model.

delta as shown in Fig. 3. In the delta, the spatial extent of the river's plume is influenced by the discharge and density gradients between the river and the gulf. The model simulates a larger plume when density gradients are considered, meaning that a less dense, turbid and buoyant plume travels farther than one with the same density of the sea. The inclusion of thermohaline processes resulted in a reduction of SSC along the west coast. The plume preventing waves from reaching the west coast may explain this unexpected result. On the other hand, when density gradients are neglected waves become the dominant process in the generation of SSC in the shallow areas of the northwest coast.

In addition to external forcings, physical parameters of the model were included in the sensitivity analysis. Details of this analysis and consideration of other parameters can be found in Velásquez and Escobar (2012) and Velásquez (2011), who found the Manning roughness coefficient, eddy viscosity and diffusivity, settling velocity, erosion parameter and critical bed shear stress for erosion to be the most important physical parameters for the computation of SSC in the gulf.

4.2. Statistical evaluation of the model

To compare measured and simulated SSC, model outputs were extracted at the grid node closest in space and time to each sampling station. The accuracy of the model to predict SSC was determined by means of the Mean Absolute Error (MAE), which is not heavily influenced by outliers; the Relative Mean Absolute Error (RMAE) and the Adjusted Relative Mean Absolute Error (ARMAE), which takes into account the Observational Error (OE) of measurements and laboratory procedures (Sutherland et al., 2004a). An OE = 4.67 mg/l was computed as the mean difference of duplicate analysis of five randomly selected water samples with different concentrations per field campaign. The statistical parameters were calculated based on equations (1)–(3), as defined by Sutherland et al. (2004a). The angular brackets denote average, vertical lines symbolize absolute values (modulus), Y and X are simulated and measured SSC, respectively.

$$MAE = \langle |Y - X| \rangle \tag{1}$$

$$RMAE = \frac{MAE}{\langle |X| \rangle} \tag{2}$$

$$ARMAE = \frac{\langle |Y - X| - OE \rangle}{\langle |X| \rangle} \tag{3}$$

4.3. Calibration

Calibration was performed during a rainy season from November 18th to December 3rd, 2011. During this period, the wind had variable directions and waves approached the study area primarily from the northeast with Hs lower than 1.5 m. The average relative humidity and temperature were 86% and 27 °C respectively. The SSC out of Atrato river mouths was approximately 90 mg/l. Details of boundary conditions used to force the calibration simulations can be found in Fig. 4. The calibration was used to determine the value of 12 unknown physical parameters in the model (See Table 1) that led to the best fit between modeled and measured superficial SSC at 78 sampling stations (see Fig. 4). Of the 12 parameters analyzed during the calibration, the Manning roughness coefficient, the critical bed shear stress, the eddy viscosity and diffusivity, and the settling velocity of fine particles were found to be essential variables to accurately reproduce observed SSC.

To represent wave exposed areas in the north and wave protected areas in the south of the gulf, a spatial calibration of settling velocities, horizontal and vertical eddy viscosity, and diffusivity coefficients was completed. The spatial variation of Manning's roughness coefficient was defined dependent on water depth and proximity to the Atrato delta, for example, a higher Manning at depths <30 m and lower Manning at deeper regions. The erosion parameter was varied spatially according to the presence of seabed vegetation on the west coast of Bahia Colombia. The final calibrated parameters are presented in Table 1.

The MAE, RMAE and ARMAE for the calibration period are 5.06 mg/l, 0.68 and 0.40 respectively. The spatial distribution of the observed and modeled SSC for the calibration period is presented in Fig. 4. This figure depicts three SSC features: (i) the highest SSC were simulated and measured, in the deltas of the Atrato, León and east coast rivers, from which the sediment is dispersed to deeper waters; (ii) intermediate SSC up to 15 mg/l were captured by the model in the northwest coast and along the east coast between Turbo and Necocli; (iii) low SSC were computed and measured in the north and along the central axis of the gulf.

Abrupt changes in SSC near the Atrato delta point out the existence of strong concentration gradients, most of them are successfully captured by the model. Gradients not captured in the simulations are likely caused by the unavailability of *in-situ* data to force the model (e.g. river discharge hydrographs and wind measurements). Despite the simplification of these parameters, most of the simulated SSC are within a factor of 2 or within the OE with respect to observations.

The values of the calibrated parameters were defined through the "One at a time" process in which the model accuracy is the main target

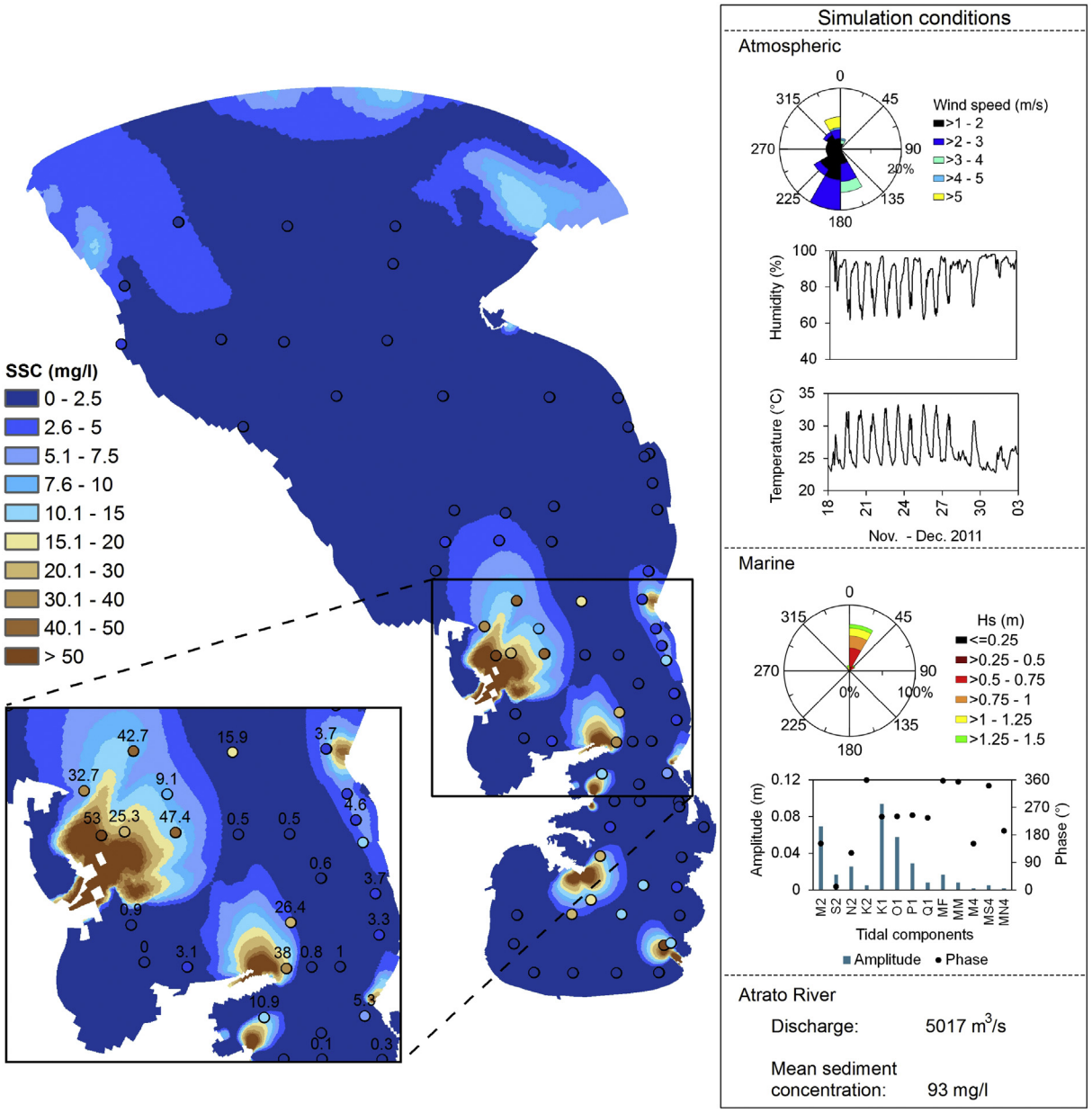

Fig. 4. Measured (dots) and modeled (background) superficial SSC and external forcings conditions during the calibration period (Nov.–Dec. 2011). Note that measurements were taken at different times and model results in the background show a single snapshot of typical SSC for the calibration period.

(Saltelli et al., 2000). This methodology allowed changing each parameter starting with the more relevant (as determined in Section 4.1) until a final model configuration generated the best fit between observations and modeled SSC. As an additional verification of the reliability of fine sediments-related parameters, their final values were compared with reported values in laboratory, field and numerical studies (Hwang and Mehta, 1989; Van Rijn, 1989; Briaud et al., 2004; Van Ledden et al., 2006; and Portela et al., 2013). It was found that calibrated values lie inside the range of reported values in different investigations.

4.4. Validation

The model validation was completed for a week in November 2010, when hurricane Tomas was passing through the Caribbean generating Hs of 2.3 m at the entrance of the Gulf of Urabá. MAE, RMAE and ARMAE were used to evaluate the performance of the model at 30 monitoring stations; 28 of which provided data at 0, 3, 5 and 10 m depth, the remaining two stations provide superficial data only. Measured and simulated SSC at different depths are presented in Fig. 5.

The range of measured SSC for the validation period varied from 3.4 to 48.4 mg/l, with the highest SSC located at the surface. The lower range of SSC with respect to the calibration period results from measurements performed far from the coast, at locations with depths exceeding 10 m. Constraints to sample shallow waters include a ship with a draft of 5 m and the choppy conditions consequence of Hurricane Tomas.

Measured water levels and waves near the model boundary (ADCP deployment) were used to force the numerical model during the validation period. It was assumed that boundary conditions from field measurements lead to a better model performance than data from global models (WWIII and TMD). To verify this assumption and to estimate the error caused by using data from global models as boundary conditions, four types of simulations forced with data from different sources were completed. The sources of tidal and wave boundary conditions for each type of simulation were: (i) field measurements; (ii) TMD and WWIII global models; (iii) TMD and wave measurements; and (iv) tide measurements and WWIII.

Table 1
Calibrated model parameters.

Type	Parameter	Value
Numerical	Grid cell	21 961
	Vertical layers	1 - 5 (2.5% of total depth each) 6 - 18 (5–7% of total depth each) 19 - 20 (2.5 and 1% respectively)
	Time step (s)	60
Physical	Wind drag coefficient at 0 m/s	0.0011
	Wind drag coefficient at 100 m/s	0.00781
	Manning Roughness coefficient	0.020 (depth < 30 m); 0.014 (depth >30 m and Atrato delta).
	Horizontal eddy viscosity (m^2/s)	100; (4.5)[a]
	Horizontal eddy diffusivity (m^2/s)	85; (3)[a]
	Vertical eddy viscosity (m^2/s)	0
	Vertical eddy diffusivity (m^2/s)	0.0085; (0.0015)[a]
	Settling velocity of cohesive sediments (mm/s)	0.5; (0.4)[a] [0.1 for 0 psμ and 0.65 for 30 psμ]
	Critical bed shear stress for sedimentation (N/m^2)	0.1 [0.12–0.52]
	Critical bed shear stress for erosion (N/m^2)	0.4 [0.1–5]
	Erosion rate coefficient ($kg/m^2/s$)	1.1×10^{-4}; (1.1×10^{-6} SW of Bahía Colombia with vegetal cover) [1×10^{-5} – 4×10^{-4}]
	Osmidov scale	0

[a] Values used for wave-exposed areas and (wave-protected areas) -North and South of Matutungo's mouth respectively. [Range of variation for cohesive parameters found in literature].

Type (i) simulation resulted in MAE = 3.53 mg/l, RMAE = 0.68 and ARMAE = 0.24. The MAE at 0, 3, 5 and 10 m depth were 5.1, 2.6, 2.6, and 3.5 mg/l respectively. The larger error at the surface is explained by the high superficial concentration at one station in front of the Matutungo mouth (indicated in Fig. 5) that was not captured by the model. If this point were to be excluded from the analysis, the MAE would have remained constant in depth. Overall, the model tended to underestimate SSC on the surface and to overestimate SSC past 5 m depth. The best accuracy was reached at 3 and 5 m depth with a MAE of 2.6 mg/l.

Comparison of type (i) and (ii) simulations indicate a 6.8% improvement on simulated SSC by forcing the model with observed tides and waves (type i) instead of using data from global models (type ii). Comparison of type (i), (iii) and (iv) simulations, indicate that observed tides account for 1.7% of improvement in model performance, while measured waves account for 5%. The effect of restricted measurements of the Atrato River discharges and winds could not be isolated nor verified, but it is expected that simplifications in these variables could lead to higher model inaccuracies due to their relevance on the dynamics of the gulf.

Results of the validation simulation indicate that the extent of the Atrato River plume was constricted and the typical northward orientation of the river's plume was shifted southwards following the direction of stronger winds and waves. Model results also indicate that nearshore currents generated by high-energy waves increased sediment transport to the south along the entire east coast, resulting in SSC comparable to those simulated in the Atrato delta. The incoming storm waves did not have major effects on SSC along the northwest coast, where bed resistance is higher due to predominantly larger sediment sizes. A similar response was found in the southwest coast of Bahia Colombia, where a lower erosion parameter was set to account for underwater vegetation effects.

High SSC modeled in near-bed layers during the validation period could not be verified due to unavailability of near-bed SSC observations. However, model results suggest the existence of hyperpycnal flows (Mulder et al., 2003; Friedrichs and Wright, 2004; Traykovski et al., 2007), which is consistent with the findings of Escobar et al. (2015), who hypothesized that these flows could exist in the Gulf of Urabá.

An additional evaluation of the model was completed for April 2010 under dry season conditions (validation 2). For this second validation period, turbidity measurements were available and SSC were defined indirectly from a correlation curve between turbidity and SSC with $r^2 = 0.77$ and mean uncertainty of 8 mg/l. The correlation curve was built from simultaneous sampling of SSC and turbidity measurements using a WPA TU140 turbidimeter. Simultaneous sampling locations correspond to measuring stations for November 2010 shown in Fig. 2.

The comparison between modeled and turbidity-originated superficial SSC resulted in MAE, RMAE and ARMAE of 6.42 mg/l, 0.81 and 0.33 respectively. Absolute and relative errors increased with respect to previous validation and calibration periods. This underperformance of the model could be partly explained by the use of a correlation instead of direct measurements of SSC. The summary of the errors for the calibration and validation periods is presented in Table 2.

4.5. Model performance

Van Rijn et al. (2002) introduced an evaluation method for hydrodynamic models with qualitative ratings for model performance. Similarly, Sutherland et al. (2004b) proposed a classification of morphological model performance based on their Brier skill scores. Such methodologies are not yet defined for sediment transport models (Winter 2007). Thus, following the evaluation methodology of Davies et al. (2002), predicted SSC are considered accurate within a factor of 2 of measured data. In accordance with this evaluation method, a graphical comparison between simulated and observed concentrations is presented in Fig. 6.

For the calibration period (rainy season), 79% of the simulated SSC fall within a factor of 2 or the OE of the measured SSC. This percentage is 87% for the first validation period (extreme event) and 38% for the second validation period (dry season). Larger inaccuracies during the second validation can be partly explained by the indirect measuring approach. Model limitations due to the lack of continuous measurements of boundary conditions and the simplified formulations for cohesive sediment transport are additional sources of errors for all the evaluation periods.

A comparison of the calibration, validation 1 and validation 2 are shown in Fig. 6. The left panel in this figure (calibration) shows a wide range of SSC values (up to 100 mg/l). During this period, measurements were performed from a small boat that allowed collection of water samples from deep waters up to very shallow areas affected by river discharges and wave action. Under the calm conditions of this period, the model accurately reproduced high SSC near river deltas (main distributaries of the Atrato and León River) and intermediate to low SSC along the east coast and deep waters respectively. Fig. 6 center and right (validation 1 and 2) show a lower range of measured SSC (up to 48 mg/l) consequence of measurements completed in deep waters relatively far from river deltas and the coastline.

Overall, the model is reasonably accurate in predicting SSC in the Gulf of Urabá. The model results concur with previous studies of sediment transport in the region (Molina et al., 1992; Chevillot et al., 1993). In addition, the statistical parameters obtained during the evaluation provide additional confidence in the model performance. However, it is noted that the accuracy of the model near the bed was not tested and it is still uncertain.

5. Seasonal sediment dynamics

One-month long simulations of the dry and rainy seasons were run to identify the seasonal variability of the SSC in the Gulf of Urabá. The length of the simulations allows investigating SSC variations within a tidal cycle and a tidal month. To observe the response of SSC during an

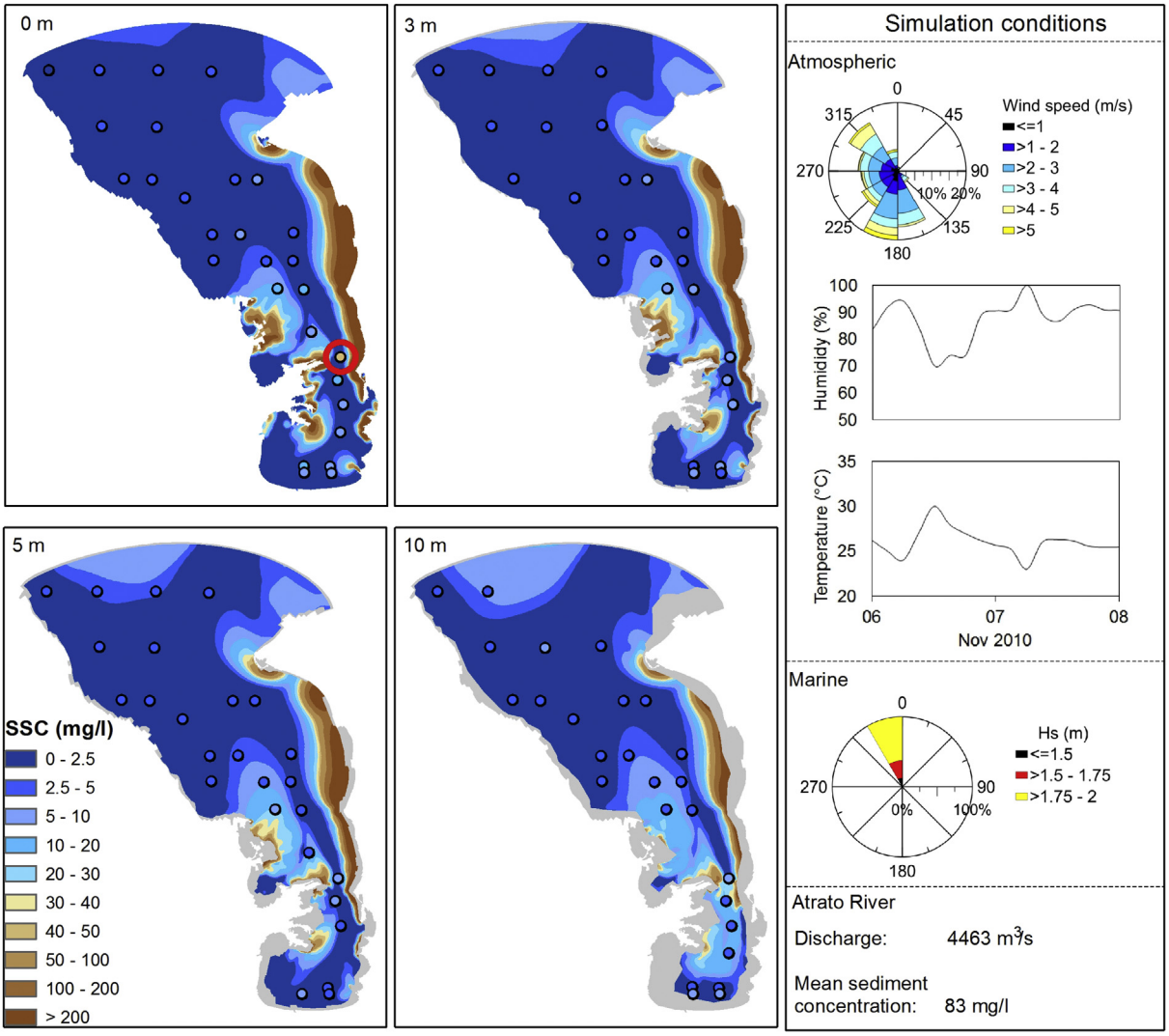

Fig. 5. Measured (dots) and modeled (background) SSC and external forcings conditions during the validation period (Nov. 2010). Note that measurements were taken at different times and model results in the background show a single snapshot of typical SSC for the validation period.

Table 2
Errors of modeled SSC in the Gulf of Urabá.

Model	Date	Depth (m)	MAE (mg/l)	RMAE	ARMAE
Calibration (rainy season)	Nov.–Dec. 2011	0	5.06	0.68	0.40
Validation (extreme event)	Nov. 2010	0	5.15	0.69	0.28
		3	2.69	0.57	0.02
		5	2.61	0.60	0.05
		10	3.56	0.85	0.25
Validation (dry season)	Apr. 2010	0	6.42	0.81	0.33

extreme event, an additional five-day simulation with high energy forcings reported in the literature (Chevillot et al., 1993; Osorio et al., 2010) was also set up. All scenarios began from hot-start simulations were hydrodynamic stability had been reached.

A summary of the boundary conditions for each scenario is presented in Table 3. Solid and flow discharges at the Atrato mouths were set to the measured values in the field campaigns at each season. For each simulation, wave and wind forcings were fixed at constant typical values, while tides, shortwave radiation, air temperature and relative humidity were set at temporally variable values.

Fig. 7 shows the superficial SSC patterns in the gulf for two seasons and an extreme event. Simulated SSC correspond to spring tide, variations of SSC within the tidal cycle (flood and ebb) and tidal month (spring and neap) were found to be of least amount, therefore, they were not included in the figure. The bottom panels in Fig. 7 correspond to the spatial extents marked by red squares in the figures at the top panels. The vectors in the bottom of Fig. 7 indicate the magnitude and direction of the superficial (rainy and dry seasons) and depth-averaged (High energy event) velocity within the gulf. Depth-averaged velocity is superimposed over the SSC on the high energy event because mix and turbulence processes are enhanced due to high winds and waves, therefore less flow stratification is expected for this scenario.

Satellite images from the Moderate Resolution Imaging Spectroradiometer (MODIS) at corresponding seasons and extreme event are also shown in Fig. 7 (middle). These images were chosen for specific days when wind and wave conditions approximately coincided to those used in the model simulations (Table 3). Because constant marine, fluvial and wind forcings were used in the simulations, a perfect fit between satellite and modeled superficial SSC was not expected. However, a qualitative good agreement between predicted and observed superficial SSC was obtained, as shown in modeled and observed patterns (A to J) in Fig. 7.

The simulation of the rainy season in combination with the satellite image allowed determining the following general SSC patterns (letters

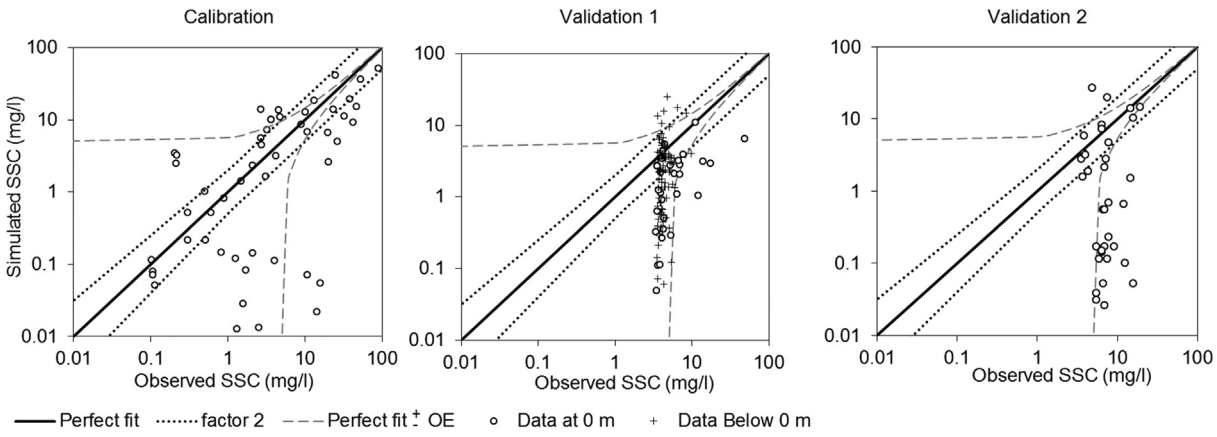

Fig. 6. Adjustment between observed and simulated SSC for the calibration period (left) and two validation periods (middle and right). Dotted lines indicate the lower and upper limits of the range of values considered accurate according to Davies et al. (2002).

Table 3
Boundary conditions to simulate dry, rainy and high energy event.

Variable	Rainy season	Dry season	High Energy Event
Mean Atrato River discharge (m^3/s) and [sediment concentration (mg/l)]	5017 [94]	4138 [83]	4138 [83]
Tarena	34 [87]	16 [125]	16 [125]
El Roto	3201 [70]	2849 [75]	2849 [75]
Pavas	11 [113]	16 [106]	16 [106]
Matuntugo	754 [76]	484 [67]	484 [67]
Coco Grande	228 [87]	138 [58]	138 [58]
Urabá	12 [46]	7 [46]	7 [46]
Leoncito	777 [107]	628 [106]	628 [106]
Wind magnitude (m/s)	3	6	8.6
Wind direction (°)	177	8	17
Significant wave height (m)	0.7	1.8	3.1
Peak wave period (s)	5	6.2	9
Wave direction (°)	29	24	22
Mean air temperature (°C)	27	25	25
Mean relative humidity (%)	81	95	95

indicate location of the pattern in Fig. 7): (A) the sediment discharge in the main mouths of the Atrato delta forms turbid plumes driven northwards by superficial currents, except by that of the Leoncito mouth, whose plume is initially driven southwards, following the orientation of its channel; (B) Wave energy concentration in headlands along the east coast enhances SSC, these sediments are driven northwards by currents that keep them in a narrow strip along the coast; (C) The discharge of the León River generates a small plume directed toward the center of Bahia Colombia; (D) sediments resuspension in the wave-exposed region of Punta Caribaná is driven by currents with a dominant northeast direction.

During the dry season and extreme event (Fig. 7 center and right), northerly winds and waves induce the following SSC patterns: (E) The León River plume gets mixed with the suspended sediments transported by the littoral drift and reaches farther into the center of Bahia Colombia. (F) The littoral drift moves southward along the east coast. This longshore current is stronger and opposite in direction to that of the rainy season. The spatial extent and magnitude of the littoral drift depend on the strength of the marine forces, but in the most energetic scenarios, it can flow almost continuously north to south from Punta Caribaná to Bahia Colombia (H and I). (G) Sediment discharge of the Atrato River typically heading north during calm weather is blocked and even turned southwards, thus suspended sediments are dispersed across the central part of the gulf. (J) Under the extreme event, the plume of the León River can merge with the littoral drift and continue moving to the southernmost part of Bahia Colombia, from where it deviates northwards due to the convergence of opposing currents.

Fig. 8 presents the modeled SSC along cross and longitudinal sections indicated in Fig. 2 for the characteristic seasons and the high energy event described in Table 3. In the rainy season, near surface SSC are generated by the plumes of the distributaries of the Atrato River. On the other hand, during high-energy events, increase of wave forces change the previous pattern and near-bed sediment transport becomes relevant.

Further analysis of differences in SSC for the two types of sediments included in the model indicate that non-cohesive SSC is usually lower than cohesive SSC during the rainy and dry seasons. However, during the high energy event, near-bed sand concentration in the northwest coast can exceed mud concentration in some grid cells near the shore. In other shallow areas like Punta Caribaná, non-cohesive sediment concentration increases significantly, attaining values up to 50% in respect to fine particles, in the Tarena Mouth and the northern coast of Turbo this ratio is only 10%.

6. Discussion and conclusions

The development of a 3D sediment transport model in a tropical estuary with scarce systematic programs to collect oceanographic, fluvial and atmospheric data was possible with overall reasonable accuracy. Statistical and qualitative evaluation of the model confirmed its fair performance and enabled the determination of seasonal SSC patterns in the gulf. During the rainy season, river plumes are the main features transporting sediments in the gulf, most of the solid discharge of the rivers is transported to the north of the mouths by buoyant jets. Energetic conditions of the dry season and extreme events in the Caribbean Sea increase SSC and reverse the sediment dynamics in the gulf. In this case, northerly winds and waves block river plumes from traveling north and enhance near bed transport and southerly littoral drift in the east coast.

The first two field campaigns in 2010 were designed to have an extensive spatial coverage of the gulf while enabling the identification of regions with high gradients of SSC. In the third and last field campaign in 2011, sampling in areas with higher SSC, like the Atrato delta and near the east coast, was increased. Future work on sediment-related studies in the gulf should focus on river deltas (El Roto, Matutungo, Leoncito and León) even if it implies a reduction of the spatial extent of samples. Under this recommendation, special attention must be given to the management of navigation risks over shallow and uncharted waters.

Numerical modeling and *in-situ* measurements were integrated to determine sediment concentration patterns in the Gulf of Urabá. This

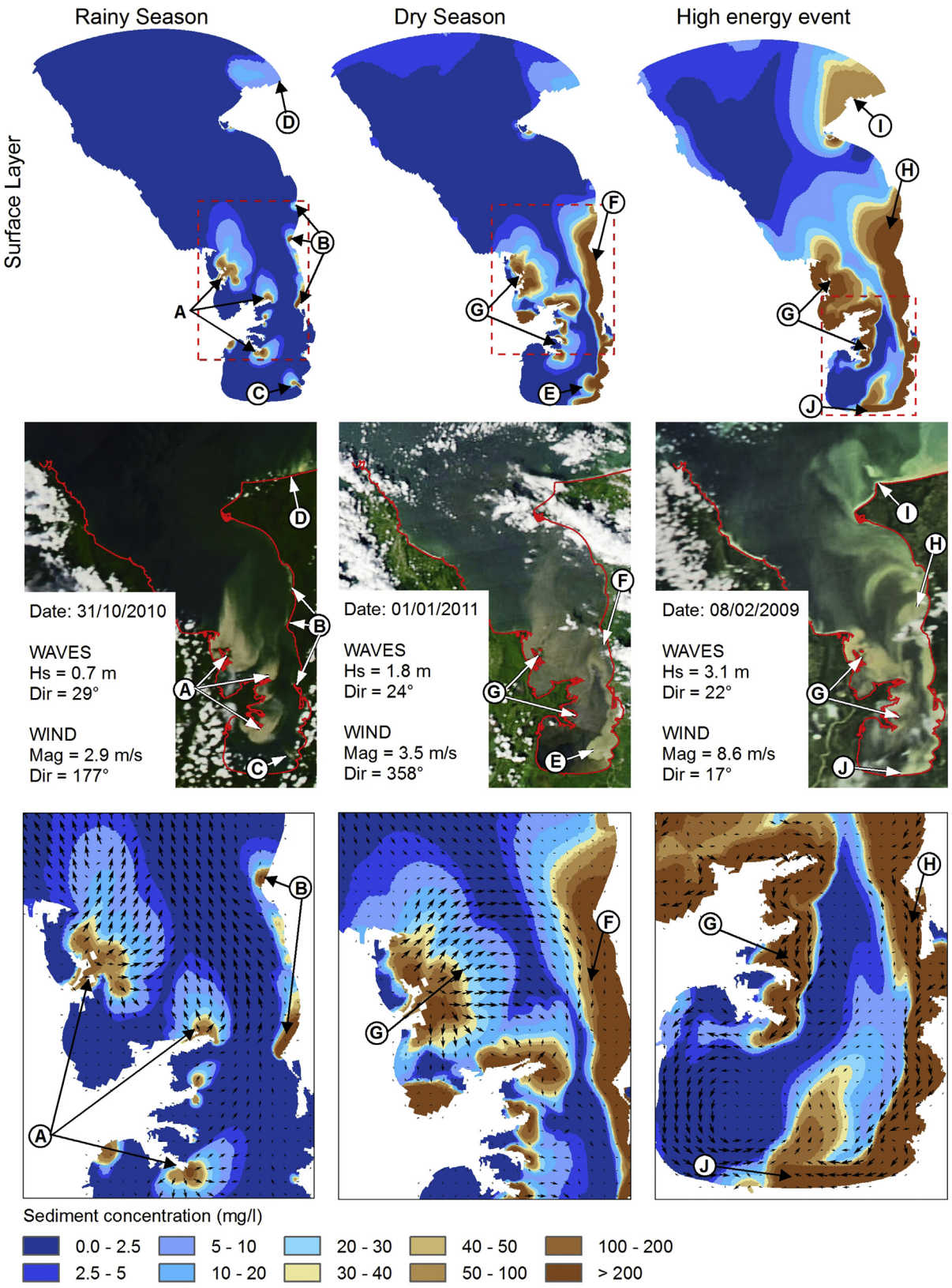

Fig. 7. Modeled SSC in the Gulf of Urabá during the rainy and dry seasons and a high energy event (Top and bottom maps). MODIS Imagery under similar forcings for each season (middle).

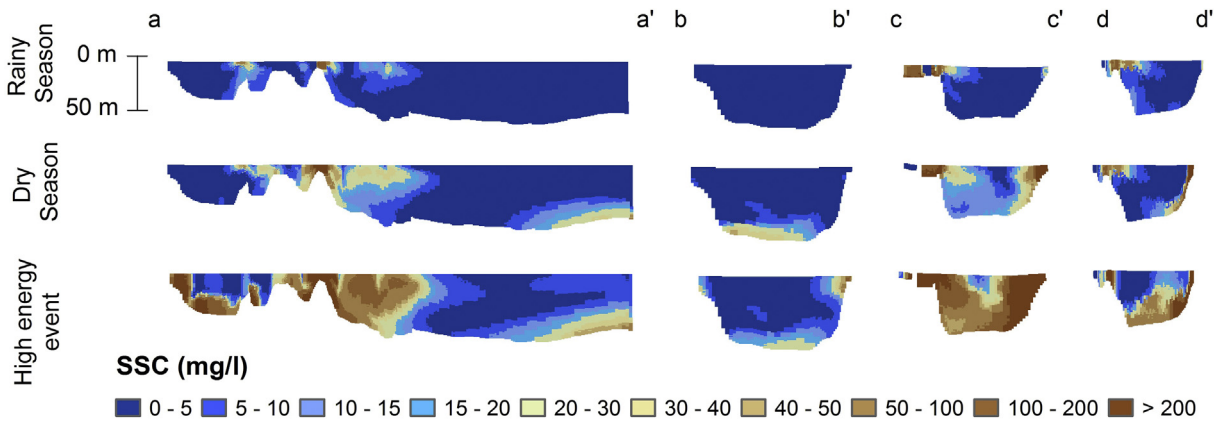

Fig. 8. Modeled SSC in cross and longitudinal sections of the Gulf of Urabá during the rainy and dry seasons and a high-energy event. Location of the sections is shown in Fig. 2.

approach worked for the rainy season, but it was not effective for energetic conditions due to reduced nearshore measurements of SSC. To overcome this issue, satellite images were incorporated in this research. These images were crucial to adjust the model for extreme oceanographic and atmospheric conditions, specifically because they led to: (i) identify the need to divide the model into wave exposed and protected areas, where independent calibration processes were required to correct excessive sediment dispersion and over prediction of superficial SSC in Bahia Colombia; (ii) reduce mud content in shallow areas of Punta Caribaná and the northwest coast, where rocks, coral reefs and coarse sediments compose the seabed; (iii) reduce the erosion factor in shallow areas of the southwest coast (Bahia Colombia), where vegetation covers the marine bed. The latter significantly reduced fine sediment entrainment and led to a better qualitative fit between modeled superficial SSC and satellite images. Limitations of satellite imagery are related to their spatio-temporal resolution. The 250 m imagery limits the detection of SSC features to scales larger than hundreds of meters. Cloud cover is also a limiting factor on the temporal availability of the images, especially when the ITCZ migrates over the gulf.

The performance of the sediment transport model was evaluated using instantaneous values of SSC measured in each field campaign at predefined stations indicated in Fig. 2. This type of model evaluation is particularly challenging because the observed SSC are the result of unsteady forcings with stochastic nature, (e.g. winds, tides, waves, thermohaline conditions and river discharges) for which *in-situ* measurements are unavailable.

Set up of boundary conditions for the sediment transport model was possible by using data from global models. Nevertheless, it should be noted that using this data to force local models, is expected to generate additional inaccuracies in the results of small-scale simulations. To quantify this additional error, comparison of model results forced with boundary conditions from both, *in-situ* measurements and global models (November 2010-validation 1) were performed. Forcing the model with observed waves and tides improves the accuracy of simulated SSC up to 6.8%. This verification could not be made for atmospheric conditions and the discharge of the Atrato River, for which *in-situ* measurements are expected to improve the model results.

Limitations of the model include the simplified formulations for cohesive sediment transport in stratified flows available in Delft3D, in which processes like flocculation and floc breakup are not fully implemented. Model results showed an important increase of near-bottom SSC during extreme events in respect to calm conditions. However, simulated near-bed SSC could not be verified due to the unavailability of near-bottom measurements. To further improve this sediment transport model, SSC sampling near the bed during high-energy events could be used to verify the formation of hyperpycnal flow, as well as, definition of bed sediment properties (e.g. size, specific density and fine content). Bathymetric measurements in the Atrato delta and regions with depths <3 m would also be useful to enhance the representation of the bottom in nearshore regions.

Acknowledgments

Field data and modeling tools used in this study were obtained from the research project: “Coastal erosion in Antioquia II: modeling of morphological evolution in the Gulf of Urabá”. The authors would like to thank the Departamento de Ciencia, Tecnología e Innovación (COLCIENCIAS), Universidad EAFIT, and the Centro de Investigaciones Oceanográficas e Hidrográficas del Caribe (CIOH) for funding this project (No. 1216-489-25530). The authors also want to thank the port authorities of Turbo for logistical support provided during the field campaigns and the anonym reviewers for their valuable comments that resulted in significant improvement on the content of this manuscript.

References

Álvarez, A.M., Bernal, G.R., 2007. Estimación del campo de transporte neto de sedimentos en el fondo de Bahía Colombia con base en análisis de tendencia del tamaño de grano. Av. Recur. hidráulicos 16, 41–50.
American Public Health Association, Water Environment Federation & Association, American Water Works, 1998. Standard Methods for the Examination of Water and Waste Water, 20 Ed. American Public Health Association, Washington, p. 1325. ISBN: 0-87553-235-7.
Bernal, G., Toro, M., Montoya, L.J., Garizábal, C., 2005. La complejidad de la dimensión física en la problemática costera del Golfo de Urabá, Colombia. Gest. Ambiente 8, 123–135.
Banco de Iniciativas Regionales para el Desarrollo de Antioquia (BIRD), 2010. Iniciativas de conexión de Antioquia con el noroccidente colombiano. BIRD, Medellín, Colombia.
Booij, N., Ris, R.C., Holthuijsen, L.H., 1999. A third-generation wave model for coastal regions, Part I, Model description and validation. J. Geophys. Res. 104, 7649–7666.
Briaud, J.L., Chen, H.C., Li, Y., Nurtjahyo, P., Wang, J., 2004. Pier and Contraction Scour in Cohesive Soils. National Cooperative Highway Research Program, NCHRP, Washington, D.C., p. 118 report 516.
Cámara de Comercio de Medellín para Antioquia, 2006. Antioquia 2020: Estrategia de competitividad para Medellín, el Área Metropolitana del Valle de Aburrá y Antioquia.
Chevillot, P., Molina, A., Giraldo, L., Molina, C., 1993. Estudio geológico e hidrológico del golfo de Urabá. Bol. Científico CIOH 14, 79–89.
CIOH, 2010. Climatología de los principales puertos del Caribe Colombiano (Turbo – Golfo de Urabá. Cartagena de Indias, Colombia).
Correa, I.D., Vernette, G., 2004. Introducción al problema de la erosión litoral en Urabá (sector Arboletes-Turbo) costa caribe colombiana. Bol. Investig. Mar. Costeras (INVEMAR) 33, 7–28.
Correa, I.D., Alcántara-Carrió, J., González, D.A., 2005. Historical and recent shore erosion along the colombian caribbean coast. J. Coast. Res. SI 49, 52–57.
Davies, A.G., Van Rijn, L.C., Damgaard, J.S., Van de Graaff, J., Ribberink, J.S., 2002. Intercomparison of research and practical sand transport models. Coast. Eng. 46, 1–23.
Deltares, 2012. Delft3D-FLOW, Simulation of Multi-dimensional Hydrodynamic Flows and Transport Phenomena, Including Sediments. User Manual. Deltares, Delft.
Egbert, G.D., Erofeeva, L., 2002. Efficient inverse modeling of barotropic ocean tides. J. Atmos. Ocean. Technol. 19, 183–204.
Escobar, C.A., 2011. Relevancia de procesos costeros en la hidrodinámica del golfo de Urabá (Caribe colombiano). Bol. Investig. Mar. Costeras – INVEMAR, St. Marta 40 (2), 327–346.

Escobar, C.A., Velásquez, L., Posada, F., 2015. Marine currents in the gulf of Urabá, colombian caribbean Sea. J. Coast. Res. 31 (6), 1363–1374.
Friedrichs, C.T., Wright, L.D., 2004. Gravity-driven sediment transport on the continental shelf: implications for equilibrium profiles near river mouths. Coast. Eng. 51, 795–811.
Galloway, W.E., 1975. Processes framework for describing the morphologic and stratigraphic evolution of deltaic depositional systems. In: Houston Geological Society, Deltas: Model for Exploration. M. L, pp. 87–98.
Hubach, E., 1930. Apreciación de los proyectos de canal interoceánico por el Napipí y el Truandó según puntos de vista geológicos. Bol. Minas Petróleo 13, 15–34.
Hwang, K.N., Mehta, A.J., 1989. Fine sediment Erodability in Lake Okeechobee, Coastal and Oceanographic Engineering Department. University of Florida, p. 140. Report UFL/COEL-89/019.
Kalnay, E., Kanamitsu, M., Kistler, R., Collins, W., Deaven, D., Gandin, L., Iredell, M., Saha, S., White, G., Woollen, J., Zhu, Y., Leetmaa, A., Reynolds, R., Chelliah, M., Ebisuzaki, W., Higgins, W., Janowiak, J., Mo, K.C., Ropelewski, C., Wang, J., Jenne, R., Joseph, D., 1996. The NCEP/NCAR 40-year Reanalysis project. Bull. Am. Meteorol. Soc. 77 (3), 437–471.
Leendertse, J.J., 1967. Aspects of a Computational Model for Long-period Water-wave Propagation. Ph.D. Thesis. Rand Corporation, Santa Monica.
Leendertse, J.J., Alexander, R.C., Liu, S.K., 1973. A Three-dimensional Model for Estuaries and Coastal Seas. Rand Corporation, Santa Monica.
Mesa, O., Poveda, G., Carvajal, L.F., 1997. Introducción al clima de Colombia. Universidad Nacional de Colombia, Sede Medellín. Facultad de Minas.
Mesinger, F., Dimego, G., Kalnay, E., Mitchell, K., Shafran, P.C., Ebisuzaki, W., Jovic, D., Woollen, J., Rogers, E., Berbery, E.H., Ek, M.B., Fan, Y., Grumbine, R., Higgins, W., Li, H., Lin, Y., Manikin, G., Parrish, D., Shi, W., 2006. North American regional Reanalysis. Bull. Am. Meteorol. Soc. 87, 343–360.
Molina, A., Molina, C., Chevillot, P., 1992. La percepción remota aplicada para determinar la circulación de las aguas superficiales del Golfo de Urabá y las variaciones de su línea de costa. Bol. científico CIOH 11, 43–58.
Montoya, L.J., Toro, M., 2006. Calibración de un modelo hidrodinámico para el estudio de los patrones de circulación en el golfo de Urabá. Av. Recur. Hidráulicos 13, 37–54.
Montoya, L.J., 2010. Dinámica oceanográfica del golfo de Urabá y su relación con los patrones de dispersión de contaminantes y sedimentos. PhD Thesis. Universidad Nacional de Colombia, Medellín.
Mulder, T., Syvitski, J.P.M., Migeon, S., Faugeres, J., Savoye, B., 2003. Marine hyperpycnal flows: initiation, behavior and related deposits. A review. Mar. Pet. Geol. 20, 861–882.
Osorio, A.F., Gómez, E.A., Álvarez, O.A., Molina, L.G., Osorio, J.D., 2010. Bases metodológicas para caracterizar el oleaje local (SEA) y de fondo (SWEll) en el Golfo de Urabá. In: Proceedings of the XXIV Latin-American Congress of Hydraulics, Punta del Este, Uruguay, November, pp. 21–25.
Partherniades, 1965. Erosion and depositation of cohesive soils. ASCE J. Hydraul. Div. 91 (HY1), 105–139.
Phillips, N.A., 1957. A coordinate system having some special advantages for numerical forecasting. J. Meteorol. 14, 184–185.
Portela, L.I., Ramos, S., Trigo-Teixeira, A., 2013. Effect of salinity on the settling velocity of fine sediments of a harbour basin. In: Proceedings 12th International Coastal Symposium (Plymouth, England). In: Conley, D.C., Masselink, G., Russell, P.E., O'Hare, T.J. (Eds.), Journal of Coastal Research, pp. 1188–1193. Special Issue No. 65, ISSN 0749-0208.
Posada, B., Henao, W., 2008. Diagnóstico de la erosión costera en el Caribe colombiano. Invemar, Ser. publicaciones Espec. 13 (Santa Marta).
Poveda, G., Mesa, O., 1997. Feedbacks between hydrological processes in tropical South American and large-scale ocean–atmospheric phenomenon. J. Clim. 10, 2690–2702.
Reniers, A.J.H.M., Roelvink, J.A., Thornton, E.B., 2004. Morphodynamic modelling of an embayed beach under wave group forcing. J. Geophys. Res. 109 (C1), 1–22.
Roelvink, J.A., Van Banning, G.K.F.M., 1994. Design and development of DELFT3D and application to coastal morphodynamics. In: Verwey, M. (Ed.), Babovic, Maksimovic, Proceedings Hydroinformatics'94. Balkema, Rotterdam, pp. 451–455.
Saltelli, A., Tarantola, S.Y., Campolongo, F., 2000. Sensitivity analysis as an ingredient of modelling. Stat. Sci. 2000 15 (4), 377–395.
Stanica, A., Dan, S., Ungureanu, V.G., 2007. Coastal changes at the Sulina mouth of the Danube River as a result of human activities. Mar. Poll. Bull. 55, 555–563.
Stelling, G.S., 1983. On the Construction of Computational Methods for Shallow Water Flow Problems. PhD Thesis. Department of Applied Sciences, Delft University of Technology.
Sutherland, J., Walstra, D.J.R., Chesher, T.J., Van Rijn, L.C., Southgate, H.N., 2004a. Evaluation of coastal area modelling systems at an estuary mouth. Coast. Eng. 51, 119–142.
Sutherland, J., Peet, A.H., Soulsby, R.L., 2004b. Evaluating the performance of morphological models. Coast. Eng. 51, 917–939.
Syvitski, J., Milliman, J., 2007. Geology, Geography, and humans battle for dominance over the delivery of fluvial sediments to the coastal ocean. J. Geol. 115, 1–19.
Thomas, Y.F., García, C., Cesaraccio, M., Rojas, X., 2007. III El paisaje en el golfo. In: García, C. (Ed.), Atlas del golfo de Urabá: una mirada al Caribe de Antioquia y Chocó. Instituto de Investigaciones Marinas y Costera y Gobernación de Antioquia, Santa Marta, Colombia, pp. 77–127.
Tolman, H.L., 1997. User Manual and System Documentation of WAVEWATCH-III Version 1.15. NOAA/NWS/NCEP/OMB Technical Note 151.
Traykovski, P., Wiberg, P.L., Geyer, W.R., 2007. Observations and modeling of wave-supported sediment gravity flows on the Po prodelta and comparison to prior observations from the Eel shelf. Cont. Shelf Res. 27 (3–4), 375–399.
Uittenbogaard, R.E., Van Kester, J.A.T.M., Stelling, G.S., 1992. Implementation of Three Turbulence Models in 3D-trisula for Rectangular Grids. Report Z81, Delft Hydraulics.
Van Ledden, M., Wang, Z.B., Winterwerp, H., De Vriend, H., 2006. Modelling sand mud morphodynamics in the Friesche Zeegat. Ocean. Dyn. 56, 248–265.
Van Rijn, L.C., 1989. Handbook of Sediment Transport by Currents and Waves. Report H461. Delft Hydraulics, Delft.
Van Rijn, L.C., 1993. Principles of Sediment Transport in Rivers, Estuaries and Coastal Seas, first ed. Aqua Publications, Delft.
Van Rijn, L.C., Walstra, D.J.R., Grasmeijer, B., Sutherland, J., Pan, S., Sierra, J.P., 2002. Simulation of nearshore hydrodynamics and morphodynamics on the time scale of storms and seasons using process-based profile models. In: Van Rijn, L.C. (Ed.), The Behaviour of a Straight Sandy Coast on the Time Scale of Storms and Seasons: Process Knowledge and Guidelines for Coastal Management, pp. S1–S33.
Van Rijn, L.C., 2007a. Unified view of sediment transport by currents and waves. I: initiation of motion, bed roughness, and bed-load transport. J. Hydraul. Eng. 133 (6), 649–667.
Van Rijn, L.C., 2007b. Unified view of sediment transport by currents and waves. II: suspended transport. J. Hydraul. Eng. 133 (6), 668–689.
Velásquez, L., Escobar, C., 2012. Spatial sensitivity analysis for a sediment transport model of the Gulf of Urabá, Colombia. In: Proceedings of the XXV Latin American Congress of Hydraulics, San Jose, Costa Rica.
Velásquez, L., 2011. Análisis de sensibilidad a un modelo de transporte de sedimentos: Golfo de Urabá, Colombia. Universidad EAFIT, p. 99.
Velasquez, C.Y., Rave, J., 1996. Dinámica costera y geomorfología en el golfo de Urabá Antioqueño. Sector boca Tarena-espiga de Turbo. Universidad Nacional de Colombia.
Velez, J., Poveda, G., Mesa, O., 2000. Balances hidrológicos de Colombia. Posgrado en Aprovechamiento de Recursos Hidráulicos).
Walling, D.E., 2006. Human impact on land–ocean sediment transfer by the world's rivers. Geomorphol. 79, 192–216.
Winter, C., 2007. On the evaluation of sediment transport models in tidal environments. Sediment. Geol. 202, 562–571.